# Lawrence Berkeley National Laboratory
## Recent Work

**Title**
Quantum Monte Carlo study of the singlet-triplet transition in ethylene

**Permalink**
https://escholarship.org/uc/item/9bk287b4

**Journal**
American Institute of Physics, 119(3)

**Authors**
Akramine, Ouafae El
Kollias, Alexander C.
Lester, William A.

**Publication Date**
2003-01-23

# Quantum Monte Carlo study of
# the singlet-triplet transition in ethylene

O. El Akramine, A. C. Kollias, and W. A. Lester, Jr.

Chemical Sciences Division, Lawrence Berkeley National Laboratory and

Department of Chemistry, Kenneth S. Pitzer Center for Theoretical Chemistry,

University of California, Berkeley, California 94720-1460.

## Abstract

A theoretical study is reported of the transition between the ground state $\left(^{1}A_{g}\right)$ and the lowest triplet state $\left(1\,^{3}B_{1u}\right)$ of ethylene based on the diffusion Monte Carlo (DMC) variant of the quantum Monte Carlo method. Using DMC trial functions constructed from Hartree-Fock, complete active space self-consistent field and multi-configuration self-consistent field wave functions, we have computed the atomization energy and the heat of formation of both states, and adiabatic and vertical energy differences between these states using both all-electron and effective core potential DMC. The ground state atomization energy and heat of formation are found to agree with experiment to within the error bounds of the computation and experiment. Predictions by DMC of the triplet state atomization energy and heat of formation are presented. The adiabatic singlet-triplet energy difference is found to differ by 5 kcal/mol from the value obtained in a recent photodissociation experiment.

# I. Introduction

Molecular electronic excited states are of great basic and technological importance. One would like the capability to predict the optical adsorption and emission spectra and other electronic properties of molecular systems. Accurate computational predictions of these properties for excited states have, however, proved more difficult to obtain than for ground states.

Ethylene is the prototypical $\pi$-electron system whose photochemical behavior is of importance in chemistry, biology and technology [1,2]. Ethylene has been studied exhaustively in the vapor and crystalline phases; earlier results have been summarized by Robin [3]. Electron energy loss spectroscopy (EELS) revealed that the $1^1 A_g \rightarrow 1^3 B_{1u}$ vertical transition occurs at 97 kcal/mol [4,5]. Electron impact spectroscopy (EIS) has established the singlet-triplet vertical excitation energy to lie in the range 97-108 kcal/mol [6].

Several large scale ab initio computational investigations of the singlet-triplet transition energy in ethylene have been carried out. The methods used in these studies were: configuration interaction with single excitations (CIS) [7,8], multi-reference CI (MR-CI) [9] and complete active space self-consistent field (CASSCF) [10].

In the present study, the electronic structure of the ground and the lowest triplet states of ethylene were examined using the diffusion Monte Carlo (DMC) method. This study is motivated by recent photodissociation studies of $C_2H_4S$ conducted at 193 nm that yielded the triplet-state heat of formation, and the adiabatic energy splitting that arises from the singlet-triplet excitation [11-13]. These experiments demonstrated the importance of combined tunable synchrotron radiation with photofragment translational spectroscopy (PTS) to yield an approach that easily distinguishes ground and first-excited states. In the approach,

product detection is carried out using soft photoionization with vacuum ultraviolet (VUV) radiation. This experimental procedure makes possible the identification of new reaction channels including one that yields the lowest triplet state of $C_2H_4$.

The ground electronic state of ethylene is a planar singlet $\left( ^1A_g \right)$ of $D_{2h}$ symmetry. Excitation of an electron from a $\pi$ bonding orbital to an $\pi^*$ anti-bonding orbital leads to a staggered equilibrium configuration in which the $CH_2$ groups are perpendicular to each other. This $90^0$ rotation is accompanied by $C-C$ bond stretching as the carbon-carbon bond converts from a double to a single bond, and results in $D_{2d}$ symmetry. This singlet-triplet transition is characterized by unfavorable Franck-Condon factors due to the geometry change [12].

The DMC method [14-16] has become an useful approach for investigating the electronic structure of molecular systems because of its potential for high accuracy and favorable scaling $(N^3)$ of the computational effort with system size N. The method has been shown to provide accurate results for the calculation of a wide range of properties, including ground state energies [17], binding energies [18], ionization potentials, and electron affinities [19]. The power of the DMC method for treating ground- and excited-state systems resides in its explicit treatment of electron-electron correlation. Highly accurate DMC calculations have been carried out for numerous systems in the ground state. There are relatively fewer studies in which excited state energies have been determined; however, see refs. 14, 20-22. Excitation energies have been described as '$\frac{1}{N}$' effects, as the change in energy is inversely proportional to the number of electrons in the system. As a result, a degree of precision must be achieved that makes possible the resolution of the energy change from the statistical uncertainty encountered in QMC calculations [23].

In this paper, we report equilibrium properties of the ground and lowest triplet states of ethylene including adiabatic and vertical energy splittings, heats of formation, and atomization energies. These quantities have been computed by the DMC method using Hartree-Fock (HF), and single-reference functions, the latter with natural orbitals (NOs) obtained from complete active space self-consistent field (CASSCF), and multi-configuration self-consistent field (MCSCF) trial functions. In addition, for comparison, Moller-Plesset second-order perturbation theory (MP2), density functional theory (DFT) in the local density approximation (LDA) and B3LYP generalized gradient approximation (GGA) results, have been carried out and are reported.

The remainder of the paper is organized as follows. Section II summarizes the quantum Monte Carlo (QMC) method and describes the trial wave functions used for the DMC calculations. In Sec. III, atomization energies, heats of formation, and singlet-triplet energy differences are reported and discussed. Section IV summarizes results and presents conclusions.

## II. Method

The DMC approach is a stochastic method for obtaining time independent solutions to the Schrödinger equation by solving the time-dependent Schrödinger equation in imaginary time [20-24]. The solution of the latter equation converges to the overall bosonic ground state. Fermion antisymmetry is introduced through the fixed-node approximation (FNA), which imposes the nodes of an approximate function $\Psi_T$ onto the unknown exact function $\Phi$. The FNA has been found to provide accurate results for ground and excited states with trial functions constructed using various ab initio basis set methods. The introduction of information on the system from another source is the essence of importance sampling [25,26], which improves convergence to the

state of interest. In the DMC method the propagation of the distribution of walkers is achieved with the short-time approximation, which provides an analytical approximation to the Green's function [27]. In the present study $\Psi_T$ is written as a product of a single determinant and a correlation function. The latter depends explicitly on interparticle coordinates. The orbitals of the single determinant in this study are NOs obtained from MCSCF and CASSF calculations using the GAMESS quantum chemistry package [28].

The form chosen for the correlation function is the 9-parameter function adapted by Schmidt and Moskowitz [29] from a function introduced by Boys and Handy (SMBH) [30]. Our DMC code includes a tenth term to satisfy the electron-nucleus cusp condition. This function contains two- and three-body terms in the form of electron-electron, electron-nucleus, and electron-other-nucleus distances. The SMBH correlation function contains first-order Jastrow terms that enable satisfying electron-electron and electron-nuclear cusp conditions [31]. Optimization of correlation function parameters is accomplished through fixed sample optimization using the absolute deviation (AD) functional [32] that minimizes the energy of $\Psi_T$ and is given by, $AD = \frac{1}{N}\sum_{i=1}^{N}\left|E_T - E_{L_i}\right|$. Here N is the number of walkers, $E_{L_i}$ is the local energy of the *ith* configuration, and $E_T$ is reference energy chosen to minimize fluctuations.

## A. DMC Trial functions

In this study, atomization energies, adiabatic and vertical energy differences between the ground singlet state and the lowest triplet state, and heats of formation of singlet and triplet $C_2H_4$ were calculated using both effective core potential (ECP) and all-electron DMC methods.

### 1. ECP trial wave functions

A soft ECP, i.e., one that is finite at the origin, in contrast to typical ECPs of quantum chemistry, is used here. Such functions yield improved efficiency of DMC calculations over previously used pseudopotentials by making possible the use of larger time steps without instabilities or noticeable bias [33,34]. A HF trial function was constructed using the uncontracted Partridge 2 basis set (16s, 11p) [35] for C and the cc-pVDZ basis set for H [36]. The Partridge C basis set was augmented by a single d-polarization function of 0.921 for the ground state and 1.013 for the triplet state.

To test the quality of the HF trial function, a CASSCF (4,8) calculation was carried out and NOs from this approach introduced into a single determinant trial function. The CASSCF (4,8) notation implies promotion of 4 electrons from the highest occupied $\pi$ and $\sigma$ orbitals into 8 active orbitals. For these calculations, we again used the modified Partridge basis set.

**2. All-electron Trial Functions**

All-electron trial functions for the ground state and the lowest triplet state were constructed using HF orbitals. The electron-nucleus cusp condition was enforced for the s basis functions. The cusp condition for these functions on C and H were satisfied using a procedure similar to one presented recently by Manten and Lüchow. [37] see Appendix. All-electron DMC energy splittings and thermochemical estimates obtained with a trial function that satisfies the electron-nucleus cusp condition and one that does not satisfy this condition are compared below and emphasize the importance of satisfying the electron-nucleus cusp condition.

**3. Other Ab Initio Calculations**

To provide an assessment of the present DMC calculations of atomization energies, heats of formation, adiabatic and vertical energy differences, we computed these quantities using the MP2, LDA and B3LYP methods at the complete basis set (CBS) limit. The CBS limit was

obtained from an exponential fit to single-point energies for the cc-pVXZ, (X=D,T, and Q) series of basis sets. These calculations were carried out using the Gaussian 98 program package [38].

## III. Results and discussion

All DMC results were obtained for geometries of the ground and triplet states optimized at the MP2 level of theory with the 6-311++G** basis set.  For the LDA and B3LYP levels of theory, the geometry was optimized using the same basis set as that used with the DMC calculations. Results of the geometry optimizations are given in Table I. The MP2 optimized ground state geometry is found to be in excellent agreement with electron diffraction [38] results. For this reason the MP2 method was also used to determine the triplet state geometry for DMC calculations.

The DMC computations were carried out with 12,800 walkers for a period long enough to obtain stochastic error bars of $\leq 0.3$ kcal/mol. There were typically 175-300 blocks and 150-200 moves per block. A small time step of $1 \times 10^{-4}$ was used to avoid zero time-step extrapolation and to guarantee a high acceptance ratio $(99.9\%)$.

### A. Atomization Energies

As a test of the DMC computational procedure for the singlet-triplet energy splitting, we calculated the atomization energy and heat of formation of $C_2H_4$ ($^1A_g$, $1^3B_{1u}$) with the method. The atomization energy is defined as the difference of the sum of the energies (valence energies with ECPs) of the atoms and the molecule including the zero point energy (ZPE),

$$E_a^{method}(C_2H_4) = 2E_{method}(C) + 4E_{method}(H) - E_{method}(C_2H_4) - E_{ZPE,method}(C_2H_4) \qquad (1)$$

7

here "method" corresponds to LDA, MP2, B3LYP, or DMC levels of theory.

The ground and excited state-atomization energies are listed in Table II. The results of the MP2 and B3LYP calculations are in good accord with experiment, while the LDA estimate overbinds by ~ 13%.

The ECP DMC ground state atomization energies are in excellent agreement with the experimental value of 531.9 kcal/mol. In particular, the HF and CASSCF soft-ECP atomization energies obtained with the Partridge basis set overlap the experimental value.

The all-electron DMC ground state atomization energy obtained with the electron-nucleus cusp correction agrees with experiment to within the error of the approaches; the means of these quantities differ by only 0.1 kcal/mol. If the cusp correction is not imposed, the computed atomization energy is 4.2 kcal/mol less than the experimental value.

The zero point energy (ZPE) of the to states was obtained using scaled harmonic frequencies at the MP2/6-311++G** level of theory. The ground state ZPE at this level of theory is in excellent agreement with experiment [40]. The ZPE for triplet $C_2H_4$, obtained from LDA, B3LYP, and MP2 calculations, was scaled by 0.96, 0.98, and 0.97 [41], respectively. For the DMC calculations, scaled MP2 ZPEs were used.

## B. Heats of formation

The heat of formation for the states of interest provides a further estimate of the accuracy of the DMC valence energies. The DMC heats of formation at 0 K and 298 K are compared in Table III to results from other ab initio methods and to experiment. The heat of formation at 298 K was determined by subtracting calculated non-relativistic atomization energies $E_a$ from the

standard experimental enthalpies of formation of the isolated atoms. The heats of formation at 0 K and 298 K were obtained from the following expressions [42].

$$\Delta H_f^0(C_2H_4) = 2\Delta H_f^0(C) + 4\Delta H_f^0(H) - E_a \qquad (2)$$

$$\Delta H_f^{298}(C_2H_4) = \Delta H_f^0(C_2H_4) - \text{TEMP} \qquad (3)$$

where TEMP is an empirical temperature correction for the interval 0 to 298 K that includes, in addition to the classical approximation for translation $\left(\frac{3}{2}RT\right)$ and rotation $\left(\frac{3}{2}RT\right)$ of the molecule, a temperature correction for the elements C and H in their standard states taken from experiment [42]. The ground state DMC heat of formation is found to be in excellent agreement with experiment for all trial functions except, as expected, with for the all-electron calculation for which the electron-nuclear cusp condition is not satisfied. This limitation leads to an overestimate of 4.25 kcal/mol for $\Delta H_f$ at 0 and 298 K.

The DMC heat of formation at 298 for the triplet-state is found to lie ~ 4kcal/mol above Qi et al.'s [12] estimate from their photodissociation experiment. Suits has indicated, however that the 3 kcal/mol error of the experiment is an underestimate given the way that the error was extracted - a procedure in which one peak was fit that was buried within another peak [43]. The DMC value is found to be in closer accord with the MR-CI results [9], differing by a ~ 2kcal/mol.

## C. Singlet-Triplet Energy Difference

Stimulated by their recent photodissociation measurements, Qi et al. suggested to us that it would be helpful to have a further theoretical estimate of the adiabatic singlet-triplet energy splitting. They obtained a value of 58(3) kcal/mol, which is to be compared with DMC values of ~66 kcal/mol obtained using ECP and all-electron DMC approaches. The discrepancy between the Qi et al. value and the DMC result may not be as large as indicated because of the procedure used to determine the experimental value [43]. One sees from Table IV that the DMC splittings lie within 0.1 kcal/mol of each other statistically so that the use of a HF or a CASSCF trial function with a soft ECP yields no numerical difference from the use of the all-electron HF trial function. These adiabatic energy differences together with the results of earlier studies and other ab initio approaches determined in this study (LDA, MP2, and B3LYP) are also listed in Table IV. The MR-CI adiabatic energy splitting [9] is found to be in closer accord with the DMC values than the results from the other ab initio approaches.

Also listed in Table IV are vertical energy splittings for each of the methods mentioned above. For this property there is a much wider experimental range of 97-108 kcal/mol. The DMC results, however, are again in similar accord at ~104 kcal/mol, with statistical differences of < 0.1 kcal/mol as found for the adiabatic energy splitting.

## Summary and Conclusions

Motivated by a recent photodissociation experiment, we have computed the adiabatic and vertical singlet-triplet energy splittings in ethylene. The DMC adiabatic splitting is found to be ~5

kcal/mol larger than a recent measurement. Other theoretical approaches (LDA, MP2, and MR-CI) also yield larger values except for B3LYP. The DMC singlet-triplet vertical energy difference and heat of formation for the triplet state at 298K are found to differ from a MR-CI result by <2kcal/mol. DMC atomization energies and heats of formation of the singlet and triplet states were found to agree with experiment to within the errors of the two approaches where experimental data is available except as noted.

**Acknowledgements**

# Appendix

The electron-nucleus (e-n) cusp condition for an ns orbital is

$$\left. \frac{\partial \ln \varphi_{ns}}{\partial r_{i\alpha}} \right|_{r_{i\alpha}=0} = -Z_{\alpha} \tag{1}$$

where $\varphi_{ns}$ in Eq. (1) refers to an $(n = 1,2,3,\ldots,)$ $s$ basis function (BF) and $Z_{\alpha}$ is the atomic number of nucleus $\alpha$. To satisfy the e-n cusp condition, we have chosen the function,

$$f_{cusp}(r_{i\alpha}) = a_1 \exp(-a_2 r_{i\alpha}) + a_3 r_{i\alpha} + a_4 \tag{2}$$

where the parameters $a_i \ \{i = 1, 2, 3, 4\}$ were determined by numerically fitting Eq. (2) to the s BF

using the Levenberg-Marquardt algorithm [44]. The e-n cusp condition written in terms of the $a_i$

fitting parameters of Eq. (2) at $r_{i\alpha} = 0$ is

$$\frac{a_3 - a_1 a_2}{a_1 + a_4} \approx -Z_\alpha \tag{3}$$

The symbol '$\approx$' in Eq. (3) is used because the fitting parameters approximate the $Z_\alpha$ to within the

error of the numeric fit.

We initially fit the exponential function of Eq. (2) to 1s and 2s BFs over an interval $[0, r_1]$,

where $r_1$ was chosen to lie at a distance sufficiently far from the nuclear center that fluctuations in

$\nabla^2 \varphi_{ns}$ have dissipated (see Fig. 1). Approximately 10,000 points were used to fit each s-BF of H

and C. This procedure was found, however, not to describe accurately the - $Z_\alpha$ behavior at the

origin. To provide greater flexibility needed to address this shortcoming, a second point, $r_2$ , is

chosen that lies closer to the nuclear center such that $0 < r_2 \ll r_1$. A least squares non-linear

regression is then carried out over the interval $[r_1, r_2]$. For C and H $r_2$ was typically set to 0.0005

Bohr. To connect $f_{cusp}(r_{i\alpha})$ smoothly to the $s$ BF and its first and second derivatives, a third-

order polynomial of the form

$$p(r_{i\alpha}) = a_0 + a_1 r_{i\alpha} + a_2 r_{i\alpha}^2 + a_3 r_{i\alpha}^3 \tag{4}$$

is introduced in the interval $[r_1, r_1 + \delta]$, where $\delta$ is a parameter typically less than 0.05

Bohr. The coefficients in Eq. (4) were determined by enforcing the continuity of the polynomial

and its first derivative at the end points of the interval $[r_1, r_1 + \delta]$. The gradient and Laplacian of

the s orbital were obtained by differentiating $f_{cusp}(r_{i\alpha})$ in the range of $[0, r_1]$ and the s orbital in

the range of $[r_3, \infty]$. Continuity of the first and second derivatives of the s BF was achieved by enforcing continuity of the connection polynomial and its first derivative at the bounds of the interval $[r_1, r_1 + \delta]$. The coefficients of $f_{cusp}(r_{i\alpha})$ and $p(r_{i\alpha})$ are listed in Table V.

The resultant function and its first and second derivatives are fit to cubic splines and the latter functions are then used in the local energy evaluation. Usually, 1000 non-equally spaced spline points were required to map the interval $[0,1]$ onto $[0,\infty]$ with the function $x_i = \alpha ih / (1 - ih)$, $i = 0,\dots,n-1$ where $h = 1/n$ and $\alpha = 0.1$.

# Literature Cited

1. M. C. Pirrung, Acc. Chem. Res. **32**, 711 **(**1999).

2. T. R Younkin, E. F.Conner, J. I. Henderson, S. K. Friedrich, R. H.Grubbs, and D. A. Bansleben, *Science* **287**, 460 (2000).

3. M. B. Robin, *Higher Excited States of Polyatomic Molecules*, Vol. 3, (Academic Press, New York, 1985).

4. D. G. Wilden, P. J. Hicks, and J. J. Comer, J. Phys. B **12**, 1579 (1979).

5. D. E. Love, and K. D. Jordan, Chem. Phys. Lett. **235**, 479 (1995).

6. E. H. Van Veen, Chem. Phys. Lett. **41**, 540 (1976).

7. J. B. Foresman, M. Head-Gordon, J. A. Pople, and M. J. Frisch, J. Phys. Chem. **96**, 135 (1992).

8. K. B. Wiberg, C. M. Hadad, J. B. Foresman, and W. A. Chupka, J. Phys. Chem. **96**, 10756 (1992).

9. B. Gemein and S. D. Peyerimhoff, J. Phys. Chem. **100**, 1925 **(**1996).

10. L. Serrano-Andres, M. Merchan, I. Nebotgil, R. Lindh, and B. O. Roos, Chem. Phys. **98**, 3151 (1993).

11. F. Qi, O. Sorkhabi, and A. G. Suits, J. Chem. Phys. **112**, 10707 (2000).

12. F. Qi, O. Sorkhabi, A. G. Suits, S. H. Chien, and W.-K. Li, J. Am. Chem. Soc. **123**, 148 (2001).

13. A. G. Suits and F. Qi, J. Electron Spectrosc. Relat. Phenom. **119**, 127  (2001).

14. B. L. Hammond, W. A. Lester, Jr., and P. J. Reynolds*, Monte Carlo Methods in Ab Initio Quantum Chemistry* (World Scientific: Singapore, 1994).

15 A. Lüchow and J. B. Anderson, Ann. Rev. Phys. Chem. **51**, 501 (2000).

16 L. Mitas and D. M. Ceperley, Adv. Chem. Phys. **93**, 1 (1996).

17. (a) C. Filippi, and C. J. Umrigar, J. Chem. Phys. **105**, 213 1996;

 (b) O. El Akramine, W. A. Lester, Jr., X. Krokidis, C. A. Taft, T. C. Guimaraes, A. C. Pavao, and R. Zhu, Mol. Phys. **101**, 277 (2003).

18. J. A. W. Harkless and W. A. Lester, Jr., J. Chem. Phys. **113**, 2680 (2000).

19. (a) R. N. Barnett, P. J. Reynolds, and W. A. Lester, Jr., J. Chem. Phys. **84**, 4992 (1986);

 (b) J. C. Grossman, M. Rohlfing, L. Mitas, S. G. Louie, and M. L. Cohen, Phys. Rev. Lett. **86**, 472 (2001)

20. (a) J. B. Anderson, J. Chem. Phys. **65**, 4121 (1976); (b) J. B. Anderson, Int. J. Quantum Chem.**15**, 109 (1979).

21. (a) P. J. Reynolds, M. Dupuis, and W. A. Lester, Jr., J. Chem. Phys. **82**, 1983 (1985);

 (b) P. J. Reynolds, R. N. Barnett, B. L. Hammond, R. M. Grimes, and W. A. Lester, Jr., Int. J. Quantum Chem. **29**, 589 (1986);

 (c) R. M. Grimes, B. L. Hammond, P. J. Reynolds, and W. A. Lester, Jr., J. Chem. Phys. **84**, 4749 (1986).

22. J. C. Grossman, W. A. Lester, Jr., and S. G. Louie, J. Am. Chem. Soc. **122**, 705 (2000).

23. W. M. Foulkes, L. Mitas, R. J. Needs, and G. Rajagopal, Rev. Mod. Phys. **73**, 33 (2001).

24. P. J. Reynolds, D. M. Ceperley, B. J. Alder, and W. A. Lester, Jr., J. Chem. Phys. **77**, 5593 (1982).

25. M. H. Kalos, D. Levesque, and L. Verlet, Phys. Rev. A **9**, 2178 (1974).

26 J. B. Anderson, Rev. Comput. Chem. **13**, 133 (1999).

27. B. L. Hammond, P. J. Reynolds, and W. A. Lester, Jr., J. Chem. Phys. **87**, 1130 (1987).

28. M. W. Schmidt, K. K. Baldridge, J. A. Boatz, S. T. Elbert, M. S. Gordon, J. H. Jensen, S. Koseki, N. Matsunaga, K. A. Nguyen, S. Su, T. L. Windus, M. Dupuis, and J. A. Montgomery, J. Comput. Chem. **14**, 1347 (1993).

29. K. E. Schmidt, and J. W. Moskowitz, J. Chem. Phys. **93**, 4172 (1990).

30. S. F. Boys, and N. C. Handy, Proc. R. Soc. London Ser. A. **310**, 43 (1969).

31. R. Jastrow, R. Phys. Rev. **98,** 1479 (1955).

32. (a) A. Aspuru-Guzik, O. Couronne, I. Ovcharenko, and W. A. Lester, Jr., **"**Deviation minimization for quantum Monte Carlo wavefunction optimization" (unpublished).

    (b) D. Bressanini, G. Morosi, and M. Mella, J. Chem. Phys. **116**, 5345 (2002).

33. C. W. Greeff and W. A. Lester, Jr., J. Chem. Phys. **109**, 1607 (1998).

34. I. Ovcharenko, A. Aspuru-Guzik, and Lester, W. A. Lester, Jr., J. Chem. Phys. **114**, 7790 (2001).

35. H. Partridge, J. Chem. Phys. **90**, 1043 (1989).

36. T. H. Dunning, J. Chem. Phys. **90**, 1007 (1989).

37. S. Manten and A. Lüchow, J. Chem. Phys. **115**, 5362 (2001).

38. Gaussian 98 (Revision A.10) M. J Frisch, G. W. Trucks, H. B. Schlegel, G. E. Scuseria, M. A. Robb, J. R. Cheeseman, V. G. Zakrzewski, J. A. Montgomery, R. E. Stratmann, J. C. Burant, S. Dapprich, J. M. Millam, A. D. Daniels, K. N. Kudin, M. C. Strain, O. Farkas, J. Tomasi, V. Barone, M. Cossi, R. Cammi, B. Mennucci, C. Pomelli, C. Adamo, S. Clifford, J. Ochterski, G. A. Petersson, P. Y. Ayala, Q. Cui, K. Morokuma, D. K. Malick, A. D. Rabuck, K. Raghavachari, J. B. Foresman, J. Cioslowski, J. V. Ortiz, A. G. Baboul, B. B. Stefanov, G. Liu, A. Liashenko, P. Piskorz, I. Komaromi, R. Gomperts, R. L. Martin, D. J. Fox, T. A. Keith, A. M. Al-Laham, C.Y. Peng, A. Nanayakkara, C. Gonzalez, M. Challacombe, P. M. W. Gill, B. G. Johnson, W. Chen, M. W. Wong, J. L. Andres, M. Head-Gordon, E. S. Replogle, J. A. Pople, Gaussian, Inc. Pittsburgh PA, 1998.

39. H. C. Allen and E. K. Plyler, J. Am. Chem. Soc. **80**, 2673 (1958).

40. M. W. Chase, Jr., C. A. Davies, J. R. Downey, Jr., D. J. Frurip, R. A. McDonald, and A. N. Syverud, *JANAF Thermochemical Tables.,* Ed. D. R. Lide, Jr., (American Chemical Society, American institute of Physics, Midland, Michigan, 1986), Vol. I, II.

41. A. P. Scott and L. Radom, J. Phys. Chem. **100**, 16502 1(996).

42. L. A. Curtiss, K. Raghavachari, P. C. Redfern, and J. A. Pople, J. Chem. Phys. **106**, 1063 (1997).

43.  A. Suits, private communication.

44. D. W. Marquardt, J. Soc. Ind. App. Math. **11**, 431 (1963).

45. J. C. Grossman, J. Chem. Phys. **117**, 1434 (2002).

Table I: Optimized structures[a] for the ground $\left({}^{1}A_{g}\right)$ and triplet $\left({}^{3}B_{1u}\right)$ states of $C_2H_4$.

| Method | $R_{C\text{-}C}(A)$ | $R_{C\text{-}H}(A)$ | HCH ($\theta$) |
|---|---|---|---|
| | | ${}^{1}A_{g}$ | |
| CIS[b] | 1.42 | 1.074 | 121.90 |
| LDA | 1.3266 | 1.0958 | 121.67 |
| MP2 | 1.3386 | 1.0848 | 121.68 |
| B3YLP | 1.3289 | 1.0850 | 121.74 |
| Experiment[c] | 1.3370 | 1.0860 | 121.19 |
| | | ${}^{3}B_{1u}$ | |
| LDA | 1.4200 | 1.1014 | 122.31 |
| MP2 | 1.4604 | 1.0847 | 121.51 |
| B3YLP | 1.4473 | 1.0880 | 121.78 |

[a]All geometry optimizations were carried out using the 6-311++G** basis set.

[b]Reference 7.

[c]Reference 40.

Table II: Atomization energies for the ground and the triplet states at their optimized geometries[a] (kcal/mol)

| Method | $C_2H_4\left(^1A_g\right)$ | $C_2H_4\left(^3B_{1u}\right)$ [b] |
|---|---|---|
| LDA | 602.39 | 536.25 |
| MP2 | 532.32 | 464.39 |
| B3LYP | 531.75 | 471.05 |
| | | |
| DMC(ECP) | | |
| MCSCF(6-311++G(2d,2p)/SBK)[c] | 533.5(4) | NA[d] |
| HF(Partridge/Soft)[e,f] | 531.67(16) | 466.50(16) |
| CASSCF(4,8)(Partridge/Soft)[f,g] | 531.73(16) | 466.19(16) |
| | | |
| DMC(all-electron) | | |
| HF(cc-pVDZ/nocusp)[h] | 527.66(56) | 469.94(59) |
| HF(cc-pVDZ/cusp)[i] | 531.80(39) | 466.59(43) |
| | | |
| Experiment[j] | 531.90(10) | NA[d] |

[a]For optimized geometries for the LDA, MP2 and B3LYP methods, see Table I.

[b]LDA, MP2, and B3LYP frequencies were scaled by 0.96, 0.98, and 0.97, see reference. [41]. The use of unscaled frequencies lead to increase in the atomization energies by 1.11 and 0.57 kcal/mol for LDA and B3LYP and 0.87 kcal/mol for MP2 and DMC results.

[c]From reference 45; a single reference trial function using natural orbitals (NOs) obtained from a MCSCF calculation with double excitations of all valence electrons into 30 virtual orbitals. The C 1s core was replaced by the SBK ECP and a basis set of the quality similar to 6-311++G(2d,2p) was used.

[d]The triplet atomization energy is not available.

[e]Trial function with HF orbitals. The C 1s core was replaced by a soft-ECP [33] and the remaining electrons were described by the Partridge [35] uncontracted basis set

[f]The Partridge uncontracted basis set for C was augmented with d-polarization functions of the cc-pVDZ basis.

[g]Single reference trial function using the NOs from a CASSCF calculation with 4 electrons distributed among 8 orbitals. The C 1s core was replaced by a soft-ECP [33] and the remaining electrons described by the Partridge uncontracted basis set.

[h]HF trial function. The electron-nucleus cusp is not enforced for the s basis functions of the cc-pVDZ basis set for C and H atoms. Statistical filtering was used to remove outliers.

[i]HF trial function. The electron-nuclus cusp is enforced for the s basis functions of the cc-pVDZ basis set for C and H atoms. See appendix for explanation.

[j]Reference 40.

Table III: Heats of formation: ground and triplet states at 0K and 298K (kcal/mol)

| Method | $\Delta H_f$ [a] | | | |
|---|---|---|---|---|
| | $^1A_g$ (0K) | $^1A_g$ (298K) | $^3B_{1u}$ (0K) | $^3B_{1u}$ (298K) |
| LDA | -55.91 | -57.94 | 10.23 | 8.53 |
| MP2 | 14.18 | 12.15 | 82.09 | 80.53 |
| B3LYP | 14.73 | 12.70 | 75.43 | 73.75 |
| MR-CI[b] | NA[c] | NA[c] | NA[c] | 76.50 |
| | | | | |
| DMC (ECP)[d] | | | | |
| HF(Partridge/Soft) | 14.79(22) | 12.76(55) | 79.96(22) | 78.40(55) |
| CASSCF(4,8)(Partridge/Soft) | 14.73(23) | 12.70(57) | 80.27(23) | 78.71(57) |
| | | | | |
| DMC(all-electron)[e] | | | | |
| HF(cc-pVDZ/nocusp) | 18.81(58) | 16.78(59) | 76.54(60) | 74.98(61) |
| HF(cc-pVDZ/cusp) | 14.68(41) | 12.65(42) | 79.88(45) | 78.32(46) |
| | | | | |
| Experiment | 14.57(07)[f] | 12.54(07)[f] | NA [g] | 70(3)[h] |

[a]Final DMC statistical errors include experimental errors in heat capacities of the atoms and molecules. For corrections using unscaled frequencies see Table II.

[b]Reference 9.

[c]Reference 9 does not report data for these quantities.
[d]For an explanation of the trial functions presented here, see footnotes a-e of Table II.

[e]For an explanation of the trial functions presented here, see footnotes f and g of Table II.

[f]Reference 40.

[g]Reference The experimental heat of formation of the triplet state at 0K is not available.

[h]Reference 12.

Table IV: $C_2H_4$ adiabatic and vertical energy differences (kcal/mol).

| Method | Adiabatic[a] | Vertical |
|---|---|---|
| CIS[b] | 46.0 | NA[c] |
| LDA | 68.1 | 112.4 |
| MP2 | 68.5 | 104.9 |
| B3LYP | 61.5 | 102.9 |
| MR-CI[d] | 64.0 | 106.0 |
| | | |
| DMC(ECP)[e] | | |
| HF(Partridge/Soft) | 66.0(3) | 104.2(3) |
| CASSCF(4,8)/Partridge/Soft) | 66.4(3) | 103.5(3) |
| | | |
| DMC(all-electron)[f] | | |
| HF(cc-pVDZ/nocusp) | 61.0(6) | NA[g] |
| HF(cc-pVDZ/cusp) | 66.3(4) | 103.8(6) |
| | | |
| Experiment | | |
| Photodissociation[h] | 58(3) | NA[g] |
| EELS[i] | NA[g] | 97 |
| EIS[j] | NA[g] | 108 |

[a]The use of unscaled frequencies changes the adiabatic energy difference by less than 0.1 kcal/mol

[b]Reference 7.

[c]Reference 7 does not report the CIS vertical excitation energy.

[d]Reference 9.

[e]For a description of the trial functions presented here, see footnotes a-e of Table II.

[f]For a description of the trial functions presented here, see footnotes f and g of Table II.

[g]Not available.

[h]Reference 12.

[i]References 4,5.

[j]Reference 6.

Table V: Cusp function fitting parameters for C and H.

| Parameter[a] | C | | H |
| --- | --- | --- | --- |
| | 1s | 2s | 1s |
| $a_1$ | 7.13566 | 0.626242 | -0.532445 |
| $a_2$ | 6.40756 | 0.923861 | 12.3077 |
| $a_3$ | -1.12723 | 0.0375271 | 4.12677 |
| $a_4$ | 0.672694 | -0.143064 | -1.24605 |

[a]Parameters for the function $a_1 \exp(-a_2 r) + a_3 r + a_4$; see Appendix.

**Figure Captions**

**Figure 1.** Electron-nucleus cusp-fitting scheme: $f_{cusp}$ is the numerically fitted exponential

function to an Gaussian type orbital (GTO).  The GTO and $f_{cusp}$ are connected by a third-order

polynomial P(r). The values $r_1$ and $r_2$ are numerically determined to satisfy the electron-nuclear

cusp condition. The value of $r_2$ is chosen to lie at a distance that fluctuations of the Laplacian of

the orbital are negligible. The interval $[r_1,r_2]$ denotes the region of the connecting polynomial

required to smoothly connect $f_{cusp}$ to the GTO.


**Figure 2.**  Cusp correction (dashed line) for the Laplacian (solid line) of the carbon 1s cc-pVDZ

basis function.  The value of $r_1$ is 0.005 bohr and for $r_2$ =1.3 bohr. The length of the polynomial

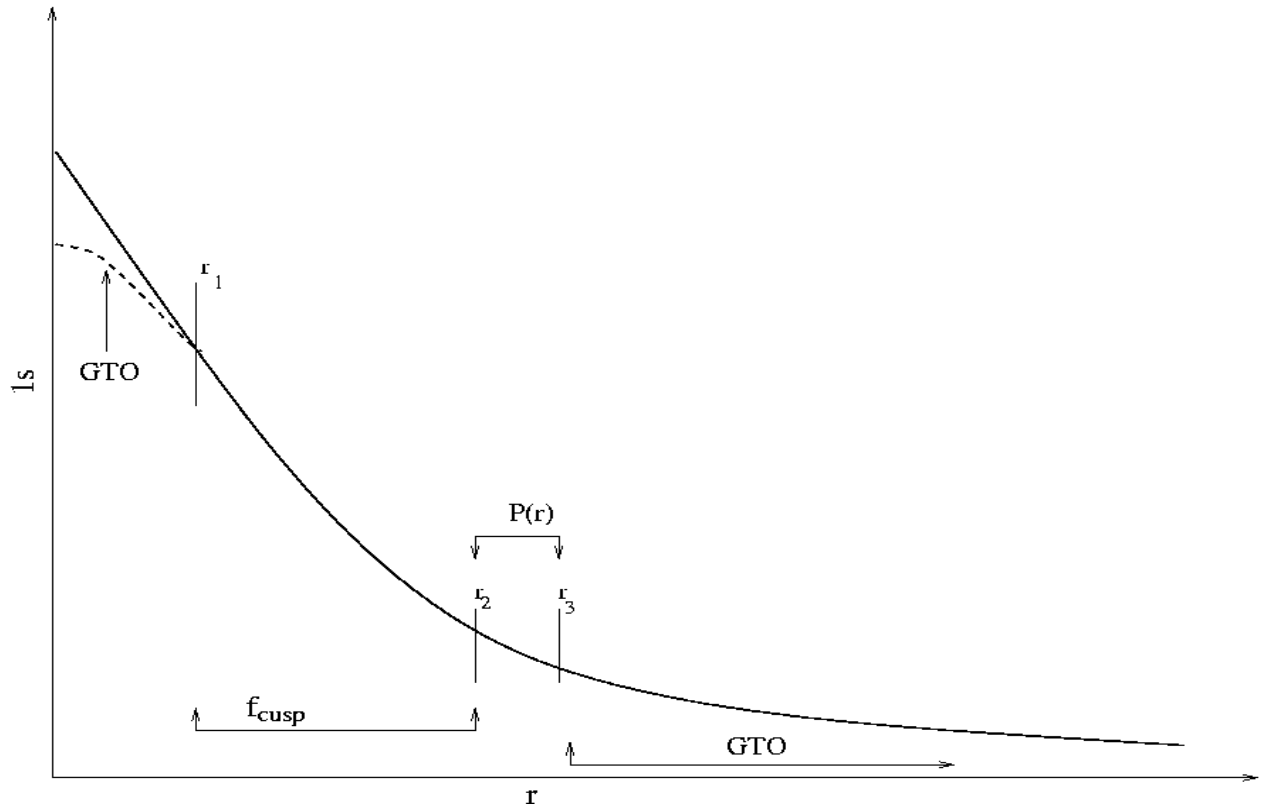connecting the electron-nuclear cusp function and the GTO, specified here as $[r_1,r_2]$  is 0.05 bohr
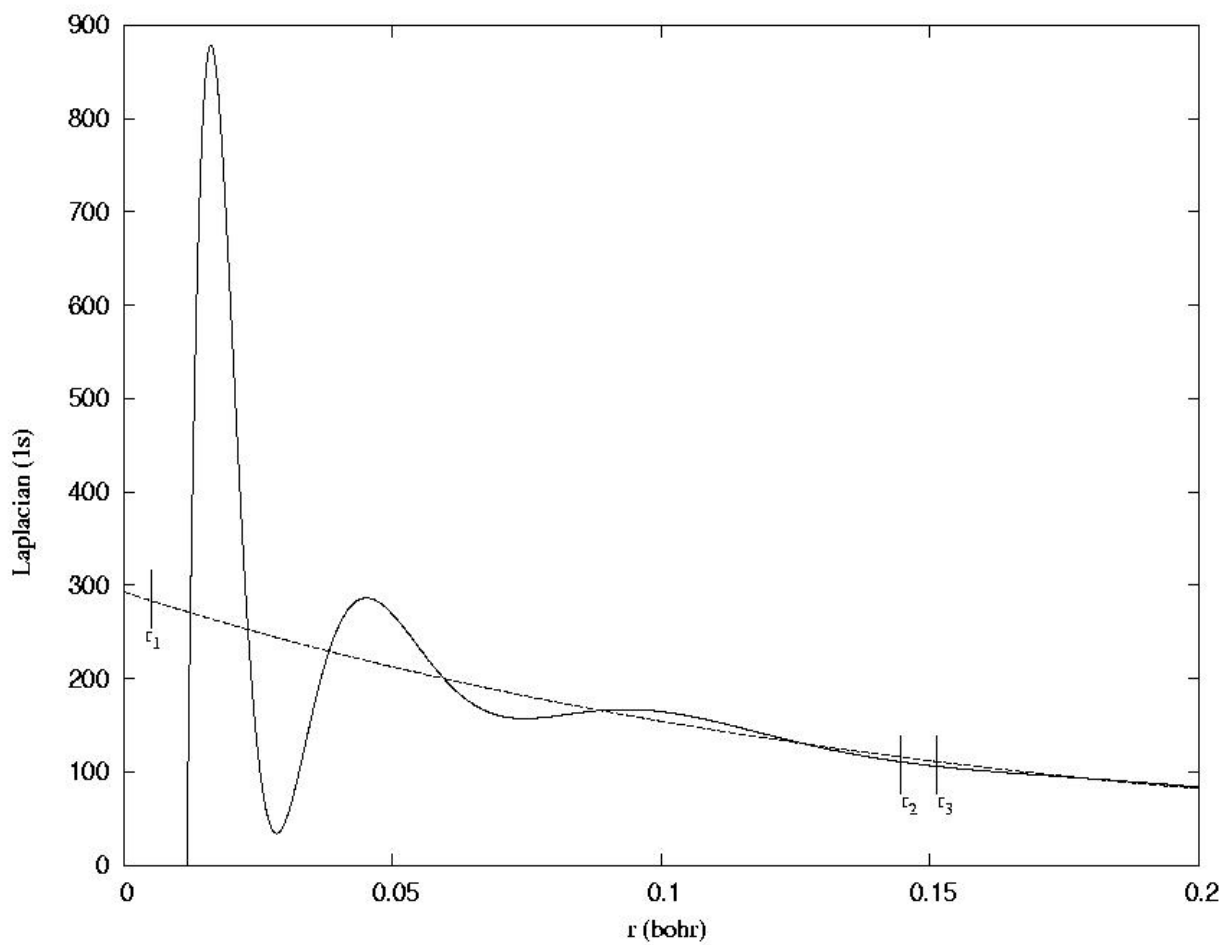
**Figure 1**

**Figure 2**